INNSPUB

Journal of Biodiversity and Environmental Sciences | JBES
ISSN: 2220-6663 (Print); 2222-3045 (Online)
Website: https://www.innspub.net
E-mail contact: info@innspub.net
Vol. 28, Issue: 6, p. 17-29, 2026

RESEARCH PAPER OPEN ACCESS

Spatiotemporal modeling of surface urban heat island and the influence of land cover changes in land surface temperature in Cagayan de Oro City, Misamis Oriental, Mindanao, Philippines

John Oliver R. Abian*, Peter D. Suson, Jaime Q. Guihawan, Hilly Ann Roa-Quiaoit, Elizabeth Edan M. Albiento

Department of Environmental Science, School of Interdisciplinary Studies, Mindanao State University, Iligan Institute of Technology, Iligan City, Philippines

Key words: Surface urban heat island, Land surface temperature, Land cover change, Spatiotemporal modeling, Remote sensing, Urban thermal environment

Received: 15 May, 2026 **Accepted:** 29 May, 2026 **Published:** 04 June, 2026

DOI: https://dx.doi.org/10.12692/jbes/28.6.17-29

ABSTRACT

Rapid urbanization and morphological transformations in Cagayan de Oro City have substantially intensified the Surface Urban Heat Island (SUHI) effect. This research quantifies the spatiotemporal evolution of the city's thermal environment from 2016 to 2024 using an empirical, multi-tiered geospatial framework. Sentinel-2A multispectral data mapped six land cover classes, validated by a simple random sampling of 300 independent points, while Landsat 8 TIRS data retrieved kinetic Land Surface Temperature (LST) via single-channel emissivity modeling. Spatial statistics expose a profound terrestrial transition, primarily driven by a 27.15% contraction of forest canopy alongside a 441.40% surge in Bare Ground and a 5.20% expansion of Built-up areas. This physical restructuring catalyzed a 2.26°C escalation in the mean basin LST. Bivariate analyses confirmed the Normalized Difference Vegetation Index (NDVI) exerts a stronger suppressive influence on LST variance (R^2= 0.4174) than the warming effect of the Normalized Difference Built-up Index (R^2= 0.3190). Translating radiometry into ecological vulnerability, the Urban Thermal Field Variance Index (UTFVI) revealed an aggressive geographic diffusion of thermal stress. Furthermore, Contribution Index (CI) assessments determined Forests are the sole remaining thermal sink, with the overall Landscape Effect Index (LI) degrading to 0.981, signaling an inverted thermal regime. Getis-Ord Gi* hotspot analysis anchored these patterns, demonstrating 67.5% of administrative units have coalesced into 99% Confidence Hot Spots. Mitigating this self-reinforcing SUHI effect demands a shift toward spatial de-clustering, strict zone to protect cold spots, and extensive green infrastructure deployment.

***Corresponding Author:** John Oliver R. Abian ✉ johnoliver.abian1010@g.msuiit.edu.ph

INTRODUCTION

Urban heat islands (UHI) represent a critical environmental challenge, characterized by significantly elevated land surface temperatures (LST) in metropolitan areas relative to their surrounding rural landscapes. This thermal contrast is fundamentally driven by rapid, uncontrolled urbanization, which replaces natural vegetation with impervious, high-density built-up zones. This physical restructuring alters surface radiation and moisture regimes by maximizing sensible heat storage and drastically reducing the latent heat flux naturally provided by evapotranspiration. In tropical and monsoon climates, such as the rapidly urbanizing Cagayan de Oro City in the Philippines, these morphological transformations are particularly severe. As the city's demographic and infrastructure footprint expands, the continuous conversion of vital forest canopies and peri-urban agriculture into highly radiant commercial zones systematically degrades the local thermal environment, intensifying heat stress and amplifying the baseline impacts of regional climate variability.

While the dynamics of Surface Urban Heat Islands (SUHI) have been extensively documented in arid regions and global megacities (Abdi, 2019; Malik and Kalotra, 2024), there remains a critical knowledge gap in quantifying these spatiotemporal thermodynamic shifts in rapidly densifying secondary tropical cities. Contemporary UHI research relies heavily on remote sensing methodologies-utilizing multispectral proxies like the Normalized Difference Vegetation Index (NDVI) and Normalized Difference Built-up Index (NDBI) derived from optical sensors to operationalize the thermal influence of vegetation versus concrete (Agrawal *et al.*, 2023; Cetin *et al.*, 2024). However, simply mapping absolute temperature increases is insufficient for equitable climate adaptation. A localized, evidence-based diagnostic framework is urgently required to move beyond raw LST mapping to structurally evaluate urban ecological stress, isolate specific land covers as thermal sources or sinks, and pinpoint the exact geographic clustering of thermal agglomerations.

Motivated by the necessity for data-driven spatial governance, this study establishes a comprehensive empirical framework to quantify SUHI dynamics in Cagayan de Oro City from 2016 to 2024. The specific aims of this research are fourfold: (1) to map the spatiotemporal transitions of a customized six-class land use and land cover taxonomy, rigorously validated via a simple random sampling of 300 independent points; (2) to determine the evolution of LST and its continuous bivariate correlation with urban morphology indices (NDVI and NDBI); (3) to assess macro-scale environmental degradation by calculating the Urban Thermal Field Variance Index (UTFVI) and evaluating landscape energy budgets via the Contribution Index (CI) and Landscape Effect Index (LI) ; and (4) to identify statistically significant spatial clusters of extreme thermal agglomeration across barangay boundaries using Getis-Ord Gi* hotspot analysis to inform targeted structural climate mitigation.

MATERIALS AND METHODS

Study area profile

Cagayan de Oro City (8° 14' to 8° 31' N, 124° 27' to 124° 49' E) encompasses approximately 412.80 km² in Northern Mindanao, Philippines (Dadole *et al.*, 2025; Cagayan de Oro City Government, 2024). The municipality is characterized by a narrow coastal plain (0–10 meters above mean sea level) along Macajalar Bay, transitioning into steeply inclined escarpments and highlands to the south (Cagayan de Oro City Government, 2024). Governed by a Type IV climate under the Modified Coronas Classification, the region lacks a pronounced dry season, experiencing peak average temperatures of 28.1 °C in May (PAGASA, 2023). The city's rapid demographic expansion and infrastructural concentration along the coastal highway corridor present a complex urban-rural gradient optimal for assessing the Surface Urban Heat Island (SUHI) phenomenon (Dadole *et al.*, 2025; UN-Habitat, 2022).

Remote sensing data procurement and pre-processing

A multi-sensor data acquisition strategy was employed utilizing 2016 and 2024 satellite imagery.

The Landsat 8 Thermal Infrared Sensor (TIRS) provided primary radiometric data via Band 10 (10.60–11.19 μm) due to its superior atmospheric transmissivity, resampled to a 30-meter spatial resolution (Sekertekin, 2020; USGS, 2020). Sentinel-2A Multispectral Instrument (MSI) data (10-meter and 20-meter bands) supplied high-precision optical indices and morphological feature extraction parameters (European Space Agency, 2022).

All datasets were projected to the Universal Transverse Mercator (UTM) Zone 51N coordinate system using the WGS 84 datum (Dadole *et al.*, 2025). Raw Landsat Digital Numbers (DN) were converted to Top-of-Atmosphere (TOA) spectral radiance applying a linear equation utilizing sensor-specific multiplicative and additive rescaling factors (USGS, 2020). Sentinel-2A data were processed to Level-2A Bottom-of-Atmosphere reflectance to eliminate aerosol scattering, while Landsat optical bands underwent atmospheric correction via the Radiative Transfer Equation (RTE) (Avdan and Jovanovska, 2016; European Space Agency, 2022). Extracted Sentinel indices were subsequently resampled to a 30-meter grid via the Nearest Neighbor method to spatially align with the thermal footprints without synthesizing artificial spectral signals (Dadole *et al.*, 2025; Sekertekin, 2020).

Spatiotemporal land covers classification and validation

Urban morphology was categorized into six taxonomic classes (Water Bodies, Forest, Crops, Built-up, Bare Ground, and Rangeland) utilizing a parametric Maximum Likelihood Classification (MLC) algorithm (Dadole *et al.*, 2025; Liping *et al.*, 2018). To ensure the structural reliability of the terrestrial baseline, independent validation was executed utilizing a simple random sampling of 300 points (Liping *et al.*, 2018). Classification accuracy was mathematically quantified through a confusion matrix, calculating the Overall Accuracy (OA) and the Kappa Coefficient (K), where a threshold of K > 0.80 confirmed high empirical reliability for subsequent thermal integration (Liping *et al.*, 2018).

LST retrieval and spectral morphology indices

Kinetic Land Surface Temperature (LST) was retrieved using a modular single-channel physical approach. Spectral radiance was converted to at-sensor brightness temperature (T_B) using Planck's radiation equation (Avdan and Jovanovska, 2016). Land Surface Emissivity (ϵ) was modeled via the NDVI Threshold Method (NDVITHM), categorizing surface graybody emissions based on the fractional vegetation cover (P_v) derived from the Normalized Difference Vegetation Index (NDVI) (Avdan and Jovanovska, 2016). The final integrated LST (T_s) was computed as follows (Avdan and Jovanovska, 2016; Sekertekin, 2020):

$$T_s = \frac{T_B}{1 + \left(\lambda \cdot \frac{T_B}{\rho}\right) \cdot \ln(\epsilon)}$$

Where λ is the emitted radiance center wavelength (10.895 \μm) and ρ is the physical constant 1.438 × 10^{-2} mK (Avdan and Jovanovska, 2016). Retrievals were cross-validated against 1-kilometer Terra/Aqua VIIRS Daily LST (VNP21A1D) data via spatial upscaling to quantify the Mean Bias Error (MBE) and Root Mean Square Error (RMSE) (Guillevic *et al.*, 2014; Li *et al.*, 2013).

To quantify morphological drivers, the Normalized Difference Built-up Index (NDBI) was calculated utilizing Sentinel-2A's Short-Wave Infrared reflectance to isolate impervious concrete materials from the vegetative baseline mapped by the NDVI (Dadole *et al.*, 2025; Faisal *et al.*, 2021).

Urban thermal indices and spatial autocorrelation

Translating absolute radiometry into ecological vulnerability, the Urban Thermal Field Variance Index (UTFVI) was applied to assess thermal degradation relative to the regional mean (Faisal *et al.*, 2021):

$$UTFVI = \frac{LST - LST_{mean}}{LST}$$

Outputs were stratified into six categorical levels from "Excellent" to "Worst" to map localized heat risk (Kafy *et al.*, 2021). The macroscopic energy budget

was concurrently evaluated using the Contribution Index (CI) to definitively classify specific land covers as thermal amplifiers (sources) or thermal buffers (sinks) based on their areal extent (S_d) and temperature differential from the municipal baseline (Zhang *et al.*, 2017).

Finally, to map the precise topological configuration of thermal stress, Getis-Ord Gi* hotspot spatial autocorrelation statistics were calculated at the barangay level (Getis and Ord, 1992).

The local statistic (Gi*) evaluates target features (x_j) within the context of neighboring spatial weights ($w_{i,j}$), generating standardized Z-scores to identify statistically significant clusters (90%, 95%, and 99% confidence intervals) of extreme thermal agglomeration (Hot Spots) or intense ecological cooling (Cold Spots) (Guerri *et al.*, 2021).

RESULTS AND DISCUSSION

Spatiotemporal dynamics of land use and land cover

The structural baseline of Cagayan de Oro's urban thermal environment is governed by its rapidly shifting physical landscape. Morphological transitions were mapped into six taxonomic categories (Water Bodies, Forest, Crops, Built-up, Bare Ground, and Rangeland) using Maximum Likelihood Classification (MLC). The empirical reliability of these classifications was confirmed through a simple random sampling of 300 independent points. The 2016 baseline achieved an Overall Accuracy (OA) of 81.67% and a Kappa Coefficient of 0.7078, while the 2024 model demonstrated enhanced robust performance with an OA of 87.67% and a Kappa Coefficient of 0.81. This exceeds the 0.80 threshold required for high-fidelity thermal integration, validating the models for subsequent environmental assessment.

Table 1. Land use land cover (LULC) Changes from 2016 to 2024

LULC class	2016 area (ha)	2016 proportion (%)	2024 area (ha)	2024 proportion (%)	Absolute change (ha)	Relative change (%)
Forest	25,627.10	58.22	18,668.20	42.41	-6,958.90	-27.15
Rangeland	8,219.20	18.67	10,239.92	23.26	+2,020.72	+24.59
Built-up	6,446.07	14.64	6,781.12	15.40	+335.05	+5.20
Crops	2,432.28	5.53	4,709.56	10.70	+2,277.28	+93.63
Bare ground	600.73	1.36	3,252.36	7.39	+2,651.63	+441.40
Water bodies	694.07	1.58	368.12	0.84	-325.95	-46.96
Total	44,019.45	100.00	44,019.28	100.00	-	-

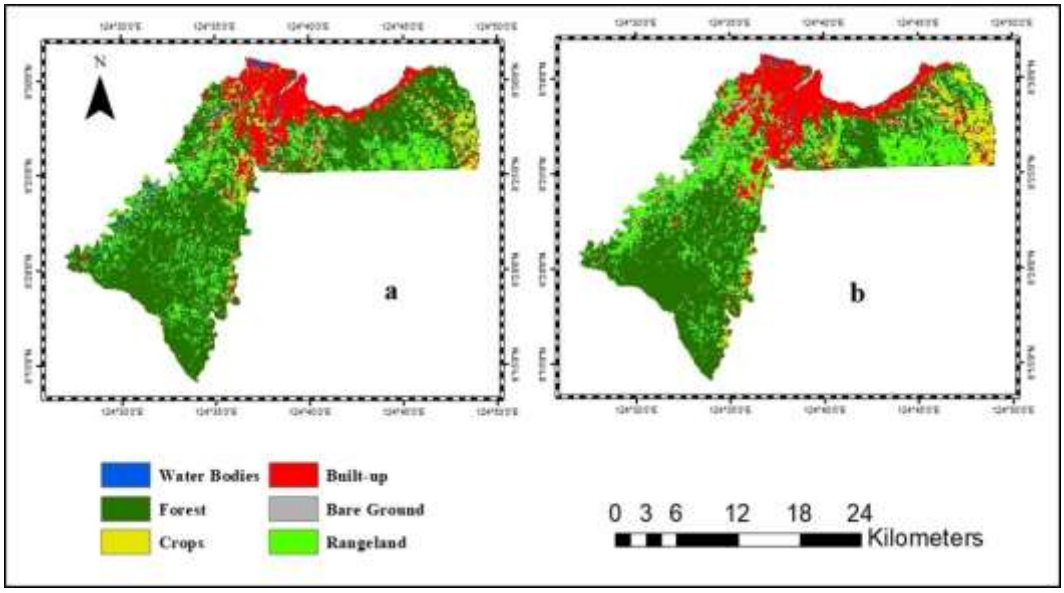

Fig. 1. Spatiotemporal land use and land cover (LULC) classification maps of Cagayan de Oro City for (a) 2016 and (b) 2024

Spatial statistics expose a landscape undergoing aggressive transitional modification between 2016 and 2024. The most critical ecological shift is the contraction of the Forest canopy, which decreased by 27.15%, translating to an absolute loss of 6,958.90 hectares. This widespread deforestation correlates directly with agricultural and transitional expansion; Bare Ground surged by 441.40% (+2,651.63 hectares) and Crops increased by 93.63% (Table 1, Fig. 1).

Simultaneously, the Built-up environment expanded by 5.20%, driven by lateral sprawl along national highway corridors and rapid coastal infilling. By substituting deeply vegetated surfaces-which naturally partition shortwave solar radiation into latent heat flux through evapotranspiration-with exposed soils and construction materials, the city has inherently disabled its regional cooling mechanisms (Abdi, 2019; Faisal *et al.*, 2021), establishing the architecture for an intensified Surface Urban Heat Island (SUHI).

Evolution of land surface temperature (LST)

The radiometric manifestation of this morphological restructuring is a definitive escalation in the thermal environment. LST fields were retrieved utilizing Landsat 8 TIRS data (Band 10), corrected for specific surface emissivity via the NDVI Threshold Method.

Basin-wide statistics confirm that the mean LST of Cagayan de Oro City increased from 32.29°C in 2016 to 34.55°C in 2024, representing an absolute ambient warming of 2.26°C (Table 2, Fig. 2).

Table 2. CDO city-wide land surface temperature statistics

LST descriptive metric	2016 (°C)	2024 (°C)	Absolute change (°C)
Minimum temperature	23.36	24.56	+1.20
Maximum temperature	50.62	50.08	-0.54
Mean basin temperature	32.29	34.55	+2.26
Standard deviation (σ)	3.14	3.51	+0.37

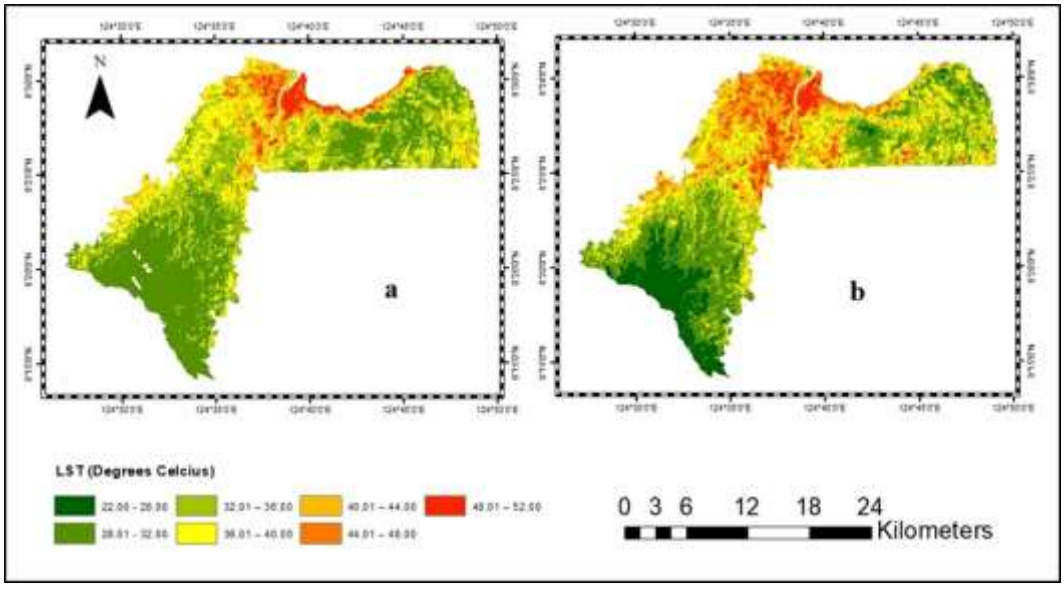

Fig. 2. Land surface temperature (LST) maps of Cagayan de Oro city for (a) 2016 and (b) 2024

Concurrently, the standard deviation of the thermal field expanded from 3.14 to 3.51. This widening variance indicates spatial thermal polarization, where the temperature divergence between the cooling forested sinks and the rapidly heating urban cores is growing increasingly extreme, a hallmark signature of SUHI intensification.

Class-wise disaggregation isolates the precise drivers of this warming. Built-up surfaces consistently registered the most intense radiometric outputs, peaking at 38.23°C in 2024 (Cetin *et al.*, 2024; Malik and Kalotra, 2024). This is governed by the high thermal admittance of asphalt and concrete, which rapidly absorb and re-radiate sensible heat.

However, the most aggressive rates of warming occurred in transitional landscapes: Rangelands surged by 3.20°C and Bare Ground by 3.02°C, illustrating the extreme localized vulnerability of unshaded, exposed soils to solar loading (Table 3).

Forests maintained their regulatory function as the coolest terrestrial surfaces (32.12°C in 2024) (Agrawal *et al.*, 2023; Faisal *et al.*, 2021), relying on multi-layered canopy shading and active evapotranspiration to dissipate radiant energy.

Table 3. Mean land surface temperature per LULC class

LULC class	Mean LST 2016 (°C)	Mean LST 2024 (°C)	Class-Specific ΔT (°C)
Built-up	37.69	38.23	+0.54
Bare ground	33.27	36.29	+3.02
Water bodies	33.52	36.25	+2.73
Crops	33.40	35.58	+2.18
Rangeland	32.26	35.46	+3.20
Forest	30.79	32.12	+1.33

Table 4. Statistical correlations of LST to NDVI and NDBI

Bivariate relationship	Pearson's r (2016)	R-squared (R^2) 2016	Pearson's r (2024)	R-squared (R^2) 2024	Statistical significance (p)
LST vs. NDVI	-0.593	0.3519	-0.646	0.4174	< 0.01
LST vs. NDBI	0.520	0.2708	0.565	0.3190	< 0.01

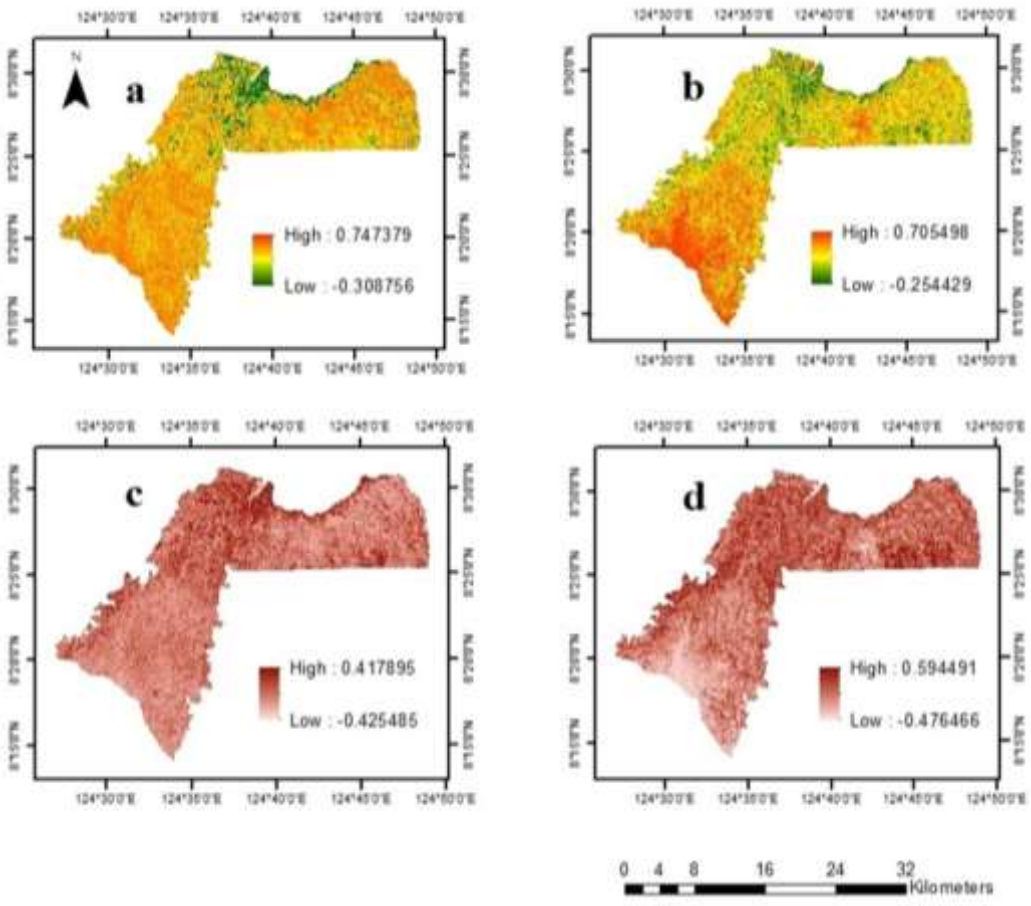

Fig. 3. Spatial distribution maps of the normalized difference vegetation index (NDVI) for (a) 2016, (b) 2024, and normalized difference built-up index (NDBI) (c) 2016, (d) 2024

To ensure radiometric integrity in the absence of dense local meteorological networks, the Landsat retrievals were cross-validated against 1-kilometer Terra/Aqua VIIRS Daily LST data. The models

yielded a Root Mean Square Error (RMSE) of 1.79°C for 2016 and 2.22°C for 2024, operating well within standard acceptable error margins for urban microclimate studies (Guillevic *et al.*, 2014). Negative Mean Bias Errors (-0.47°C to -0.92°C) accurately reflected natural diurnal solar accumulation between the morning Landsat and afternoon VIIRS overpasses.

Bivariate correlation to urban morphology

To quantitatively map the continuous statistical relationship between surface temperatures and physical land cover, bivariate Pearson correlations (r) and coefficients of determination (R^2) were evaluated for LST against the Normalized Difference Vegetation Index (NDVI) and the Normalized Difference Built-up Index (NDBI) (Table 4, Fig. 3-4).

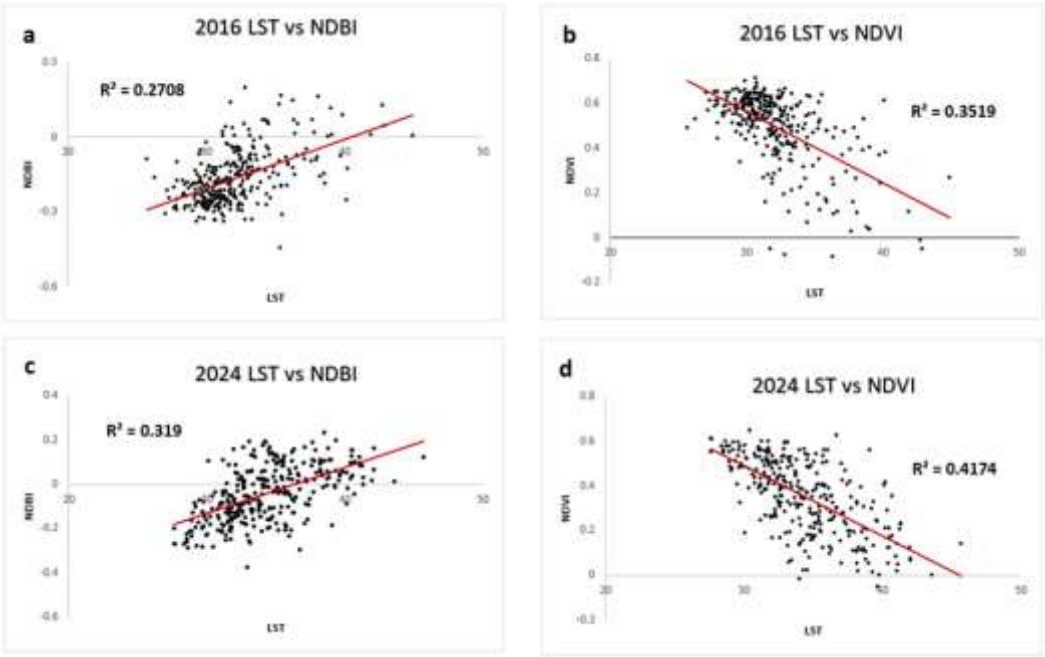

Fig. 4. Scatterplots showing bivariate correlation of LST to NDBI and NDVI for (a, b) 2016 and (c, d) 2024

The analysis revealed a highly significant ($p < 0.01$) positive correlation between LST and NDBI, indicating that 31.90% of spatial temperature variance (R^2= 0.3190) in 2024 is explained by the concentration of impervious concrete materials. However, the inverse relationship between LST and NDVI demonstrated notably stronger explanatory power, tightening from R^2= 0.3519 in 2016 to R^2= 0.4174 in 2024. The strengthening of this negative correlation over the eight-year period proves that as the broader urban basin aggressively warms, the localized cooling effect of remaining intact vegetation becomes mathematically more pronounced. These metrics validate that preserving vegetation (NDVI) exerts a structurally stronger suppressive influence on thermal extremes than the warming effect driven by concrete expansion (NDBI).

Spatiotemporal Evolution of Ecological Stress (UTFVI)

Absolute radiometric temperatures do not fully capture human thermal comfort or environmental degradation (Kafy *et al.*, 2021; Faisal *et al.*, 2021). Consequently, LST was normalized using the Urban Thermal Field Variance Index (UTFVI) to assess relative ecological stress across Cagayan de Oro's 80 barangays (Table 5, Fig. 5).

The spatial distribution of UTFVI reveals a profound morphological shift categorized by thermal decentralization. In 2016, extreme ecological stress was hyper-concentrated in the highly impervious northern coastal Central Business District, leaving 34 barangays in a state of "Phenomenal" (Worst) SUHI intensity. By 2024, this localized peak fragmented; the number of

barangays experiencing phenomenal stress dropped to 14. However, this reduction in the urban core was offset by a massive geographic diffusion of intermediate heat into peri-urban and eastern corridors. Barangays classified under "Middle," "Strong," and "Stronger" SUHI intensities surged from a combined 21 to 46. Concurrently, the city lost the majority of its transitional ecological buffers, with "Weak" (Good) stress barangays plummeting from 12 to 5. This dynamic explicitly tracks the horizontal sprawl of the city, wherein outward infrastructural development distributes intense thermal loads into formerly resilient, vegetated frontiers.

Table 5. Spatiotemporal shift of mean UTFVI and SUHI intensity by Barangay

Mean UTFVI threshold	Ecological evaluation	SUHI intensity	2016 (No. of Barangays)	2024 (No. of Barangays)	Net change
< 0.00	Excellent	None	13	15	+2
0.00 – 0.05	Good	Weak	12	5	-7
0.05 – 0.10	Normal	Middle	4	10	+6
0.10 – 0.15	Bad	Strong	8	17	+9
0.15 – 0.20	Worse	Stronger	9	19	+10
> 0.20	Worst	Phenomenal	34	14	-20
Total			80	80	

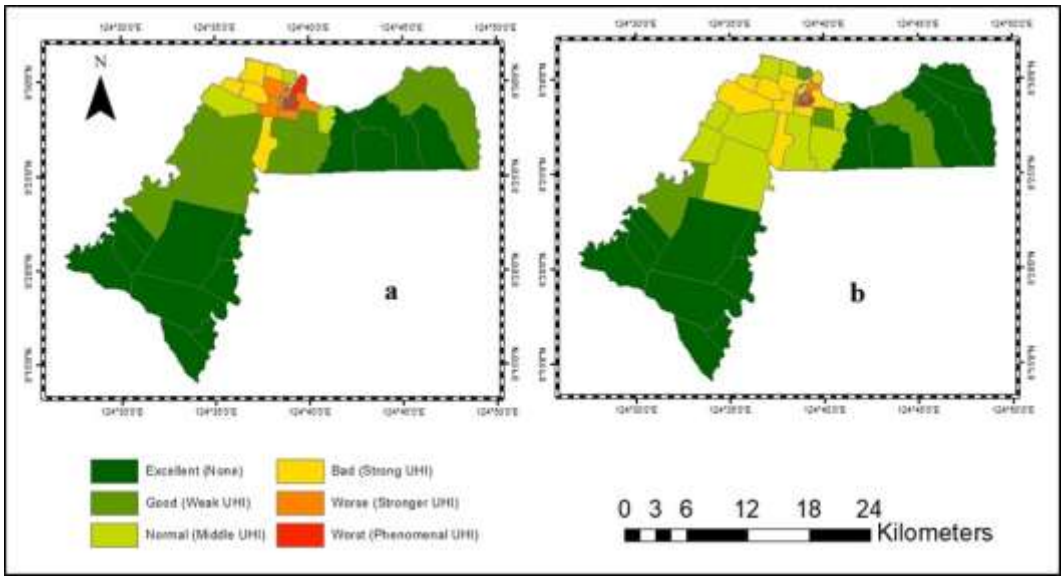

Fig. 5. Comparative Barangay-level urban thermal field variance index (UTFVI) and SUHI intensity maps of Cagayan de Oro City for (a) 2016 and (b) 2024

Contribution (CI) and landscape effect (LI) indices

The relative impact of specific morphological features on the regional thermal environment was quantified using the Contribution Index (CI) (Zhang *et al.*, 2017) (Table 6, Fig. 6).

Built-up areas persist as the most potent thermal amplifier per hectare (Zhang *et al.*, 2017), maintaining high positive CI values (+0.792 in 2016; +0.522 in 2024). Due to vast areal expansion, the warming contributions of Bare Ground (+0.119) and Crops (+0.103) have also escalated significantly. Rangelands underwent a functional transition; acting as a marginal thermal sink in 2016 (-0.005), their rapid desiccation converted them into a potent heat source (+0.198) by 2024.

Forests represent the municipality's singular, overwhelming thermal sink (Zhang *et al.*, 2017). Despite the 27.15% reduction in total area, the forest CI deepened to -0.937. This occurs because the thermal disparity between the remaining cool forests and the rapidly escalating basin-wide mean has

widened; the surviving canopies are mathematically strained to offset regional warming. The macro-scale Landscape Effect Index (LI) contextualizes this thermodynamic imbalance. In 2016, the LI was calculated at 0.988, indicating the city was already operating below the required 1.0 equilibrium threshold. By 2024, the LI degraded further to 0.981. Cagayan de Oro currently exists in an inverted thermal regime where anthropogenic heat sources structurally overpower the restorative cooling capacity of the natural landscape, shifting the SUHI effect into a self-reinforcing, city-wide hazard.

Table 6. Class contribution index (CI) and landscape roles

LULC Class	2016 CI value	2016 landscape role	2024 CI value	2024 landscape role
Built-up	+0.792	Thermal source	+0.522	Thermal source
Bare Ground	+0.014	Thermal source	+0.119	Thermal source
Crops	+0.062	Thermal source	+0.103	Thermal source
Water Bodies	+0.019	Thermal source	+0.013	Thermal source
Rangeland	-0.005	Thermal sink	+0.198	Thermal source
Forest	-0.871	Thermal sink	-0.937	Thermal sink

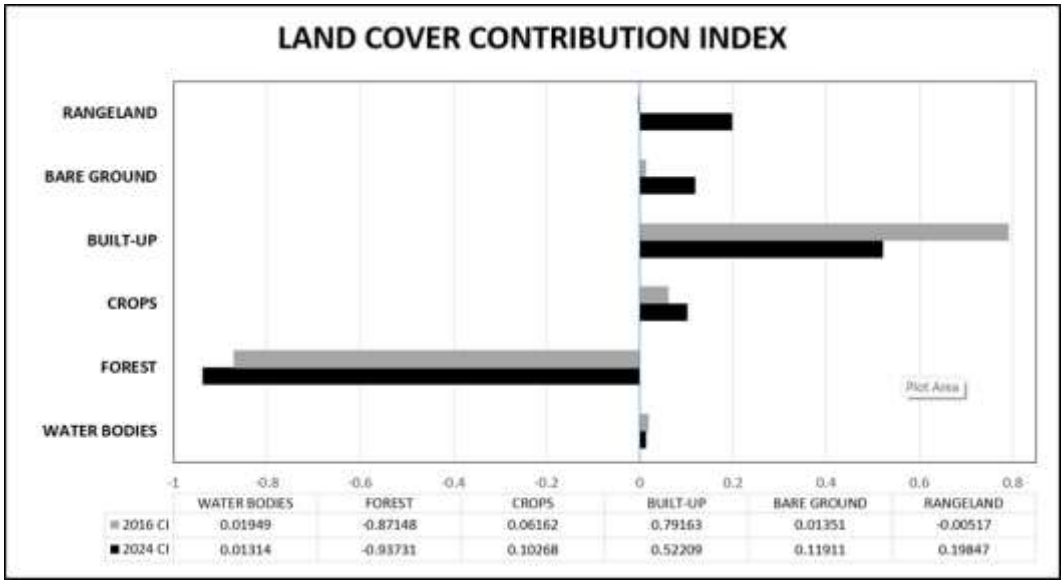

Fig. 6. Land cover contribution index (CI) bar chart

Spatial autocorrelation and thermal clustering

To determine if observed thermal patterns constitute statistically significant agglomerations, a Getis-Ord Gi* Hotspot Analysis was executed.

The Gi* outputs visualize a massively contiguous Hot Spot cluster dominating the northern and western administrative units. By 2024, a staggering 67.5% of the city's administrative units (54 of 80 barangays) coalesced into 99% Confidence Hot Spots. This near-total lack of intermediate (90% or 95%) warming zones dictates that the urban core is locked in a state of severe thermal retention. When high-value features are densely surrounded by similarly radiant neighbors, the localized capacity to dissipate overnight heat is artificially neutralized (Getis and Ord, 1992; Guerri *et al.*, 2021) (Table 7, Fig. 7).

Furthermore, the city's transitional cooling zones entirely collapsed; 90% Confidence Cold Spots dropped from 5 to 0 between the epochs, confirming an extreme ecological polarization where only the deepest, unbroken forest blocks in the southern hinterlands maintain statistically significant regional cooling.

Mitigating this autocorrelated urban heat mass requires aggressive spatial de-clustering. Localized aesthetic interventions will be rapidly overwhelmed

by the contiguous thermal neighborhood. Stabilizing the urban climate necessitates the insertion of large-scale green infrastructure corridors to physically fracture the statistical contiguity of the northern Hot Spots, accompanied by strict zoning enforcement to prevent the southward encroachment of impervious development into the city's final remaining thermal regulators.

Table 7. Spatiotemporal evolution of thermal hot spots and cold spots

Gi_Bin value	Spatial cluster type	2016 (No. of Barangays)	2024 (No. of Barangays)	Net change
+3	Hot Spot (99% Confidence)	53	54	+1
+2	Hot Spot (95% Confidence)	1	1	0
+1	Hot Spot (90% Confidence)	0	0	0
0	Not Significant	5	8	+3
-1	Cold Spot (90% Confidence)	5	0	-5
-2	Cold Spot (95% Confidence)	15	12	-3
-3	Cold Spot (99% Confidence)	1	5	+4
Total		80	80	

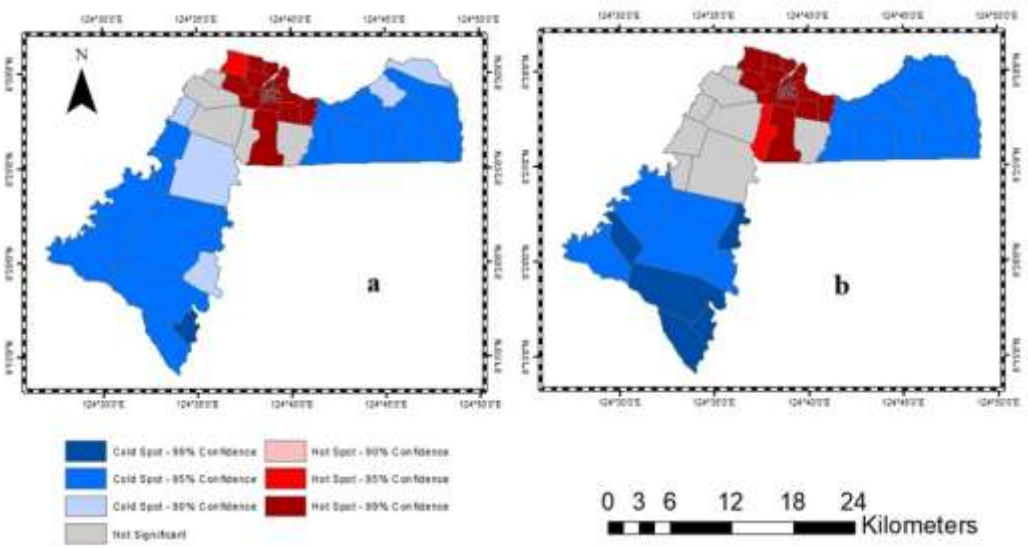

Fig. 7. Getis-Ord Gi* spatial hot spot and cold spot maps

CONCLUSION

Cagayan de Oro City is undergoing severe, systematic thermal degradation driven by the unmitigated conversion of its natural landscape. Between 2016 and 2024, the loss of 6,958 hectares of forest canopy catalyzed an inverted thermal regime, evidenced by a Landscape Effect Index degrading below the equilibrium threshold to 0.981. The Surface Urban Heat Island (SUHI) effect is no longer confined to the highly impervious central business district; it has aggressively diffused into peri-urban corridors. Spatial statistics confirm that 67.5% of administrative units have coalesced into 99% Confidence Hot Spots, actively neutralizing the city's remaining ecological buffers. Because the Normalized Difference Vegetation Index (NDVI) structurally dictates spatial temperature variance, reversing this self-reinforcing systemic hazard requires an immediate paradigm shift. Local governments must pivot from reactive environmental management to proactive, data-driven spatial governance to stabilize the rapidly warming urban climate.

RECOMMENDATIONS

Policy and spatial planning interventions

To effectively lower urban temperatures, planning strategies must immediately abandon highly localized, small-scale aesthetic greening. Because the urban heat island operates as a massively contiguous statistical cluster, the local government must implement aggressive spatial de-clustering.

This requires the insertion of large-scale green infrastructure corridors designed specifically to physically fracture the contiguity of northern Hot Spots.

Furthermore, the remaining contiguous cold spots-particularly the upland forests and critically fragmented riparian corridors in the southern hinterlands-must be fiercely protected. Their thermodynamic function as the city's final remaining absolute thermal sinks is physically irreplaceable. This protection must be enforced through strict zoning regulations, conservation easements, and definitive urban growth boundaries.

In the hyper-dense commercial core where lateral space for reforestation is virtually non-existent, surgical structural interventions are required. The city government must integrate mandatory high-albedo (reflective) roofing materials and permeable pavements into the building codes for all new commercial and industrial developments. These materials directly suppress the absorption of shortwave radiation and manipulate localized built-up parameters.

Finally, spatial planners must deploy a legislative firewall by enforcing strict land use zoning in "Not Significant" transitional barangays to arrest the southward encroachment of extreme thermal agglomerations.

FUTURE RESEARCH

To transition from diagnostic observation to predictive urban management, future academic research should integrate historical remote sensing datasets into a Cellular Automata-Artificial Neural Network (CA-ANN) framework, mirroring methodologies successfully applied in comparable tropical megacities. Simulating the spatial trajectories of impervious surface expansion will allow researchers to forecast the exact geographical distribution of the SUHI footprint for 2032 and beyond, establishing a foundation for preemptive municipal zoning.

Second, subsequent studies must bridge the gap between absolute radiometric temperatures and lived human experience. Research should prioritize the integration of in situ socio-economic demographics, localized air temperature measurements, and atmospheric humidity indices. This multi-variable approach will accurately map the direct impacts of thermal exposure on public health, thermal comfort, and environmental equity.

Finally, the academic community should establish a continuous, multi-sensor temporal monitoring architecture. By incorporating high-revisit instruments, such as MODIS or Sentinel-3, alongside high-resolution Landsat data, researchers can capture short-term phenological shifts and seasonal monsoonal variations. This will provide a more granular, dynamic understanding of the urban heat footprint throughout the calendar year.

ACKNOWLEDGEMENTS

The completion of this research would not have been possible without the profound support and contributions of numerous institutions and individuals.

First and foremost, I extend my deepest gratitude to the Department of Science and Technology – Science Education Institute (DOST-SEI) for the invaluable financial support provided through the Accelerated Science and Technology Human Resource Development Program (ASTHRDP). This scholarship grant was instrumental in sustaining my academic journey and facilitating the rigorous spatial analyses and resource-intensive modeling required for this study.

I also wish to acknowledge the Department of Environmental Science under the School of Interdisciplinary Studies at Mindanao State University – Iligan Institute of Technology (MSU-IIT) for fostering an intellectually stimulating and supportive academic environment throughout the duration of my graduate studies.

Furthermore, this study relied on the accessibility of global earth observation data. I gratefully acknowledge the United States Geological Survey (USGS) and the European Space Agency (ESA) for the public provision of the Landsat 8 Thermal Infrared Sensor (TIRS) and Sentinel-2A multispectral satellite imagery, respectively, which served as the foundational datasets for the spatiotemporal analysis of Cagayan de Oro City.

Finally, to my family, colleagues, and friends, whose moral support, understanding, and relentless encouragement fueled my persistence throughout the complexities of this research endeavor.

REFERENCES

Abdi AM. 2019. Decadal land-use/land-cover and land surface temperature change in Dubai and implications on the urban heat island effect: A preliminary assessment. EarthArXiv.

Agrawal Y, Pandey H, Tiwari PS. 2023. Analytical study of relation between land surface temperature and land use/land cover using spectral indices: A case study of Chandigarh. Journal of Geomatics **17**(2). DOI:10.58825/jog.2023.17.2.65.

Avdan U, Jovanovska G. 2016. Algorithm for automated mapping of land surface temperature using LANDSAT 8 satellite data. Journal of Sensors **2016**, 1–8. DOI: 10.1155/2016/1480307.

Cagayan de Oro City Government. 2024. Enhanced Local Climate Change Action Plan (ELCCAP) 2022–2031. City Planning and Development Office.

Cetin M, Ozenen Kavlak M, Anil Senyel Kurkcuoglu M, Ozturk GB, Cabuk SN, Cabuk A. 2024. Determination of land surface temperature and urban heat island effects with remote sensing capabilities: The case of Kayseri, Türkiye. Natural Hazards **120**.
DOI: 10.1007/s11069-024-06431-5.

Dadole JT, Companion KS, Albiento EE, Masalig R. 2025. Spatio-temporal analysis of land use and land cover change and its impact on land surface temperature in Cagayan de Oro City. Journal of World Development **6**, 52.

European Space Agency (ESA). 2022. Sentinel-2 MSI technical guide. ESA Sentinel Online.

Faisal AA, Kafy AA, Al Rakib A, Akter KS, Jahir DMA, Sikdar MS, Rahman MM, et al. 2021. Assessing and predicting land use/land cover, land surface temperature and urban thermal field variance index using Landsat imagery for Dhaka Metropolitan Area. Environmental Challenges **4**, 100192.
DOI: 10.1016/j.envc.2021.100192.

Getis A, Ord JK. 1992. The analysis of spatial association by use of distance statistics. Geographical Analysis **24**(3), 189–206.
DOI: 10.1111/j.1538-4632.1992.tb00261.x.

Guerri G, Crisci A, Messeri A. 2021. Thermal hot-spot and cool-spot analysis using Landsat 8 LST data related to 2015–2019 summer daytime periods. Remote Sensing **13**(3), 538.
DOI: 10.3390/rs13030538.

Guillevic PC, Biard JC, Hulley GC, Privette JL, Hook SJ, Olioso A, Radocinski RG, et al. 2014. Validation of land surface temperature products derived from the Visible Infrared Imaging Radiometer Suite (VIIRS) using ground-based and heritage satellite measurements. Remote Sensing of Environment **154**, 19–37.
DOI:10.1016/j.rse.2014.08.013.

Kafy AA, Al Rakib A, Akter KS, Rahaman ZA, Faisal AA, Mallik S, Ali MY, et al. 2021. Monitoring and forecasting the impact of urbanization on the thermal environment of Addis Ababa City, Ethiopia. Environmental Challenges **4**, 100170.

Le HT, Pham VT, Tran XB, Nguyen VT, Vu XC, Tong TH, Le VP. 2024. Mapping impervious surface change from remote sensing and GIS data: A case study in Ho Chi Minh City, Vietnam. Ecological Questions **35**(3).
DOI: 10.12775/EQ.2024.030.

Li ZL, Tang BH, Wu H, Ren H, Yan G, Wan Z, Sobrino JA. 2013. Satellite-derived land surface temperature: Current status and perspectives. Remote Sensing of Environment **131**, 14–37.

Liping C, Yujun S, Saeed S. 2018. Monitoring and predicting land use and land cover changes using remote sensing and GIS techniques: A case study of a hilly area, Jiangle, China. PLOS ONE **13**(7), e0200493.

Malik A, Kalotra G. 2024. Land surface temperature and urban heat island: A case study of Faridabad City using RS and GIS techniques. International Journal for Multidisciplinary Research **6**(1).

PAGASA. 2023. Climatological data for Lumbia Airport, Misamis Oriental (1991–2023). Department of Science and Technology.

Sekertekin A. 2020. Performance of land surface temperature retrieval algorithms: A case study of Landsat 8 TIRS. Environmental Science and Pollution Research **27**(12), 12345–12356.

UN-Habitat. 2022. Achieving sustainable urban development: Cagayan de Oro City. UN-Habitat Philippines.

USGS. 2020. Landsat 8–9 Operational Land Imager/Thermal Infrared Sensor Level-2, Collection 2. U.S. Geological Survey.
DOI: 10.5066/P9OGBGM6.

Zhang Y, Sun L, Hu L. 2017. Estimating the contribution of different land use/land cover types to urban heat island intensity. Remote Sensing **9**(1), 17.